5ICEGE
5th International Conference on Earthquake Geotechnical Engineering
January 2011, 10-13 | Santiago, Chile
Paper No. ATTVO

A TRANSLATIONAL THEOREM FOR YIELDING SYSTEMS

Elia VOYAGAKI [*], George MYLONAKIS [†], Ioannis N. PSYCHARIS [3]

ABSTRACT

A new scaling property is presented for the response of yielding systems to dynamic loading. Existing scaling laws are invariably *multiplicative* in nature, relating peak dynamic response to products of key problem parameters such as the linear spectral coordinates, the force reduction coefficient and the peak values of the excitation and its time derivatives. Contrary to these laws, the proposed property is *additive*, leading to a shift in the ordinates and abscissa of the excitation function by means of a pair of parameters uniquely related to the yielding resistance and the vibrational characteristics of the system. The dynamic response is then obtained by integrating the modified excitation time history in a linear manner, with the nonlinearity embedded into the forcing term. A broad class of systems, ranging from rigid-perfectly plastic to bilinear, are examined and the mathematical validity of the property is demonstrated by means of basic calculus. The significance of the property is highlighted for the important case of sliding blocks under near-field earthquake motions affected by forward fault-rupture directivity. It is shown that the ordinates and the duration of the modified excitation function may be significantly smaller than those of the original ground motion depending on the properties of the dynamic system. This reduction applies to all ground motion parameters (acceleration, velocity, displacement), but it is more pronounced for the displacement component.

Keywords: *scaling, yielding response, closed-form solution, near-fault motion, pulse, analysis*

INTRODUCTION

Most scaling laws for yielding oscillators (Veletsos & Newmark 1960, Miranda & Bertero 1994) naturally involve *multiplicative* relations between excitation and response parameters for various linear and yielding

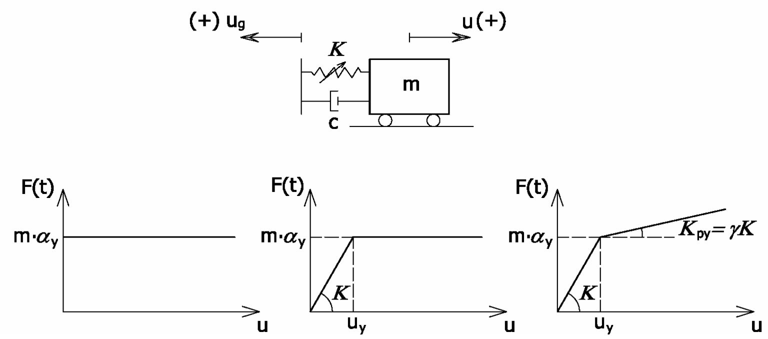

Figure 1. Idealized yielding systems considered in this study. From left to right: (a) Rigid-perfectly plastic, (b) Elastic – perfectly plastic, (c) Bilinear.

[*] Ph.D. Candidate, School of Civil Engineering, National Technical University, Athens, Greece, e-mail: eliavoyager@hotmail.com
[†] Associate Professor, Department of Civil Engineering, University of Patras, Greece
[3] Associate Professor, School of Civil Engineering, National Technical University, Athens, Greece

systems. For the latter type of systems, a different class of scaling laws, *additive* rather than multiplicative in nature, can be developed as explained in the ensuing. It will be shown that this property is general and can be of importance for high-intensity, low-cycle loading such as that induced by near-fault earthquake motions affected by forward fault rupture directivity.

A. Rigid-Perfectly Plastic System

For the reference ordinates of Fig 1, the equation of motion after yielding of a rigid perfectly-plastic system subjected to ground acceleration $\ddot{u}_g(t)$ can be written as

$$\ddot{u} + a_y \operatorname{sgn}(\dot{u}) = +\ddot{u}_g(t) \qquad (1)^{\ddagger}$$

in which $u = u(t)$ denotes displacement relative to ground and *sgn*( ) the signum function. For simplicity and without loss of generality, one may assume positive system velocity during a particular response branch; the above equation can be integrated twice for displacement to read

$$u(t) = u_g(t) - \frac{1}{2}\left(t - t_y\right)^2 a_y - \left(t - t_y\right)\dot{u}_{gy} - u_{gy} \qquad (2)$$

where u_g, $\dot{u}_{gy}$ stand, respectively, for ground displacement and velocity at yielding ($t = t_y$). Note that due to rigidity, the relative velocity and displacement of the system at yielding have been assumed to be zero.

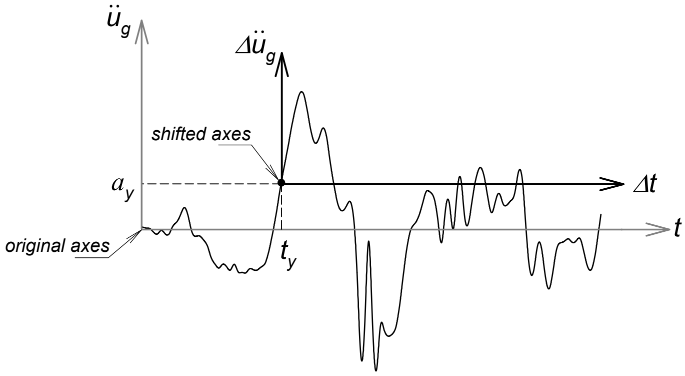

Figure 2. Translation of axes for a rigid – perfectly plastic system.

A difficulty associated with the interpretation of Eq. (2) is that the right-hand side depends on a large number of terms, that do not scale uniformly with ground acceleration and yielding resistance. In addition, the response appears to depend on the "snapshot" ground motion parameters u_{gy} and $\dot{u}_{gy}$ which are difficult to incorporate in design formulas to be used in routine engineering calculations. Moreover, the influence of the second of these parameters on the solution appears to be unreasonably strong, for it is multiplied by time, thereby its contribution tends to dominate in long signals. Evidently, a naive integration of Eq. (1), like the one in Eq. (2), although mathematically rigorous, might not be suitable for revealing the underlying physics and, thereby, possible scaling laws of the response of the system at hand. A simpler alternative can be obtained as shown below.

By virtue of the definitions of the shifted ground motion parameters,

‡ The positive sign in the right-hand side of Eq. (1) is to ensure positive response $u(t)$ for positive ground acceleration $\ddot{u}_g(t)$, as evident from the reference axes of Fig 1.

$$\Delta t \equiv t - t_y \tag{3}$$

$$\Delta u_g(t) \equiv u_g - u_{gy} \tag{4}$$

$$\Delta \dot{u}_g(t) \equiv \dot{u}_g - \dot{u}_{gy} \tag{5}$$

$$\Delta \ddot{u}_g(t) \equiv \ddot{u}_g - a_y \tag{6}$$

and the pair of integral properties (Voyagaki 2011),

$$\Delta u_g = \int_0^{\Delta t} \Delta \dot{u}_g dt + \dot{u}_{gy}\, \Delta \mathrm{t} \ , \qquad \Delta \dot{u}_g = \int_0^{\Delta t} \Delta \ddot{u}_g dt + a_y\, \Delta \mathrm{t} \tag{7-8}$$

it is straightforward to show that Eq. (2) can be written in the simpler form

$$u = \int_0^{\Delta t} \Delta \dot{u}_g dt - \frac{1}{2} a_y \Delta t^2 \tag{9}$$

For a rigid-plastic system, $a_y = \ddot{u}_{gy}$; the above result can further simplify to

$$u = \int_0^{\Delta t}\int_0^{\Delta t} \Delta \ddot{u}_g dt^2 \tag{10}$$

This remarkably simple expression suggests that the displacement response of the system can be obtained by integrating twice ground acceleration shifted by an amount equal to the yield acceleration without regard for initial conditions. In other words, the yielding resistance and the initial conditions can be incorporated into the excitation function by simply translating the origin of axes from point (0, 0) to point (a_y, t_y), thereby replacing co-ordinates ($\ddot{u}_g$, t) by ($\Delta\ddot{u}_g$, Δt), as shown in Fig (2). Evidently, Eq. (10) can be viewed as a superior solution to Eq. (2), for it is compact and does not involve the snapshot ground motion parameters u_g and $\dot{u}_{gy}$. In light of these developments, the time history $\Delta\ddot{u}_g(t)$ in Eq. (6) will be referred hereafter to as *plastic input acceleration (PIA)* for it is uniquely associated with the post-yielding response of the system. It must be emphasized that $\Delta\ddot{u}_g(t)$ is not the derivative of $\Delta\dot{u}_g(t)$, nor is $\Delta\dot{u}_g(t)$ the derivative of $\Delta u_g(t)$ as suggested by Eqs (7) and (8).

B. Elastic-Perfectly Plastic Oscillator

The post-yielding response of an undamped elastic-perfectly plastic system (Fig 1) can be described by the equation (Veletsos & Ventura 1984, Bracewell 1986)

$$\ddot{u} + a_y \,\mathrm{sgn}(\dot{u}) = \ddot{u}_g(t) + \delta(t - t_y)\,\dot{u}_y + \dot{\delta}(t - t_y)\,u_y \tag{11}$$

in which $\delta(t)$, $\dot{\delta}(t)$ denote the delta function and its first derivative (doublet function), respectively. u_y and $\dot{u}_y$ stand, respectively, for the relative displacement and velocity of the system at yielding. The advantage of using Eq. (11) over conventional formulations is evident as the differential operator and the initial conditions can be written on the same line.

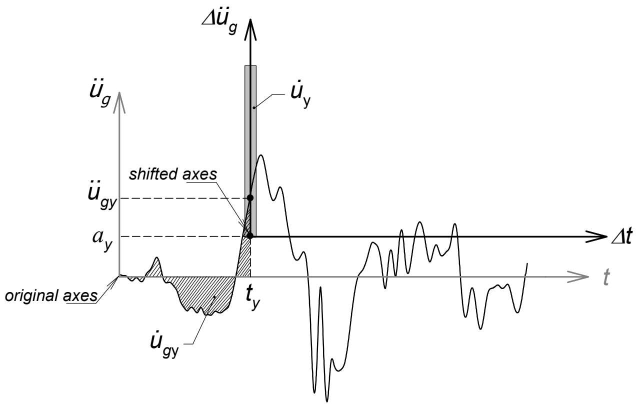

Figure 3. Translation of axes for an elastic-perfectly plastic system. Shaded areas correspond to initial conditions at yielding.

In the same spirit as in the previous system, assuming positive system velocity and integrating twice with respect to time yields the solution

$$u = u_g - \frac{1}{2}\left(t - t_y\right)^2 a_y - \left(t - t_y\right)\dot{u}_{gy} - u_{gy} + \left(t - t_y\right)\dot{u}_y + u_y \tag{12}$$

where u_{gy}, $\dot{u}_{gy}$ have the same meaning as before.

It has already been shown that the first four terms in the right-hand side of Eq. (12) can be re-arranged as

$$u = u_y + \left(t - t_y\right)\dot{u}_y + \int_0^{\Delta t}\int_0^{\Delta t} \Delta\ddot{u}_g \, dt^2 \tag{13}$$

where $\Delta\ddot{u}_g$ can be interpreted in terms of Eq. (6).

Introducing the plastic displacement

$$\Delta u \equiv u - u_y \tag{14}$$

and incorporating oscillator velocity at yielding under the integral sign, Eq. (13) can be written in the more compact form

$$\Delta u = \int_0^{\Delta t}\int_0^{\Delta t} [\Delta\ddot{u}_g + \dot{u}_y \; \delta\left(t - t_y\right)] \, dt^2 \tag{15}$$

This result suggests that the post-yielding displacement of the elastic-perfectly plastic oscillator can be obtained, as before, by integrating twice the shifted ground acceleration, $\Delta\ddot{u}_g = \ddot{u}_g - a_y$, plus a velocity impulse centered at $t = t_y$ (Fig 3). The additional term over Eq. (10) is due to the non-zero relative oscillator velocity at yielding, a feature that does not exist in the rigid-plastic system. Note that setting u_y and $\dot{u}_y$ equal to zero, the above expression duly reduces to Eq. (10). It is also noteworthy that the modified acceleration function $\Delta\ddot{u}_g$ is not zero at $t = t_y$, for ground acceleration $\ddot{u}_g$ at yielding is generally different from a_y (Fig 3).

C. Bi-linear Yielding System

The post-yielding response of a simple damped oscillator with bi-linear force-displacement characteristics (Fig 1c) is governed by the equation (Voyagaki 2011)

$$\ddot{u} + 2\omega_n^* \zeta^* \dot{u} + \omega_n^{*2} u = +\ddot{u}_g(t) - (1-\gamma)\alpha_y \,\mathrm{sgn}(\dot{u}) + \delta(t - t_{yi})\dot{u}_{yi} + [\dot{\delta}(t - t_{yi}) + 2\zeta^* \omega_n^* \delta(t - t_{yi})]u_{yi} \tag{16}$$

where

$$\gamma = \frac{K_{py}}{K}, \quad \omega_n^* = \sqrt{\frac{\gamma K}{m}}, \quad \zeta^* = \frac{c_{py}}{2\omega_n^*} \tag{17-19}$$

denote, respectively, the post-yielding hardening parameter, natural period and damping of the oscillator, respectively. In the above equation, i denotes the particular yielding branch while functions $\delta(t)$, $\dot{\delta}(t)$ and parameters u_y, $\dot{u}_y$ have the same meaning as before. Note that ω_n^* should not be viewed as a conventional natural frequency, for it is not constant over a complete oscillation cycle of the non-linear system.

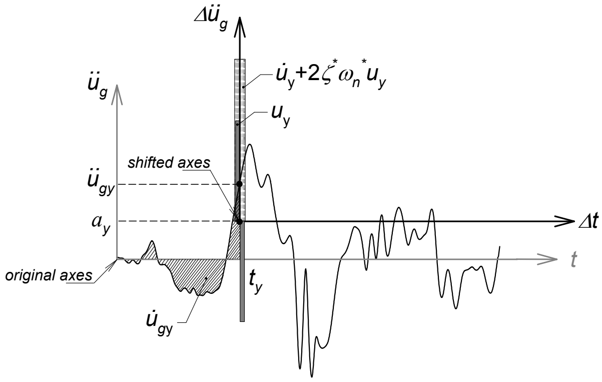

Figure 4. Translation of axes for a bilinear yielding system. Shaded areas correspond to initial conditions at yielding.

Introducing $\Delta t = t - t_{yi}$ and $\Delta u = u - u_{yi}$, index i referring to the particular yielding branch, Eq. (16) takes the form

$$\Delta\ddot{u} + 2\omega_n^* \zeta^* \Delta\dot{u} + \omega_n^{*2} \Delta u = \ddot{u}_g(t) - (1-\gamma)\alpha_y \,\mathrm{sgn}(\dot{u}) - \omega_n^{*2} u_{yi} + \delta(\Delta t)\dot{u}_{yi} + [\dot{\delta}(\Delta t) + 2\zeta^* \omega_n^* \delta(\Delta t)]u_{yi} \tag{20}$$

Moreover, introducing $u_{yi} = \chi_i u_y$, χ_i being a dimensionless constant and substituting $\omega_n^{*2} u_{yi} = \gamma \chi_i a_y \,\mathrm{sgn}(\dot{u})$ in the right hand side of Eqn (20) one obtains:

$$\Delta\ddot{u} + 2\omega_n^* \zeta^* \Delta\dot{u} + \omega_n^{*2} \Delta u = +\Delta\ddot{u}_g(t) + (1-\chi_i)\gamma\alpha_y \,\mathrm{sgn}(\dot{u}) + \delta(\Delta t)\dot{u}_{yi} + [\dot{\delta}(\Delta t) + 2\zeta^* \omega_n^* \delta(\Delta t)]\chi_i u_y \tag{21}$$

The solution to Eq. (21) can be expressed in terms of the convolution integral.

$$\Delta u = \int_0^{\Delta t} \left\{ \Delta\ddot{u}_g(\tau) + (1-\chi_i)\gamma a_y + \delta(\tau)\dot{u}_{yi} + [\dot{\delta}(\tau) + 2\zeta^* \omega_n^* \delta(\tau)]\chi_i u_y \right\} h(\tau)\,\mathrm{d}\tau \tag{22}$$

where $h(\tau)$ denotes the kernel (Bracewell 1986)

$$h = \frac{1}{\omega_D^*} \exp[-\zeta^* \omega_n^* (\Delta t - \tau)] \; \sin[\omega_D^* (\Delta t - \tau)] \tag{23}$$

where $\omega_D^* = \omega_n^* \sqrt{1-\zeta^{*2}}$ is the corresponding damped cyclic natural frequency and Δt is given by Eq. (3).

The *plastic* excitation function of the bilinear system is equal to the shifted ground acceleration $\Delta\ddot{u}_g$, plus a set of impulsive terms related to the initial conditions at yielding (Fig 4).

Accordingly, in the remainder of this paper the integrals $\int \Delta\ddot{u}_g\, dt$ and $\int\int \Delta\ddot{u}_g dt^2$ will be simply referred to as *plastic input velocity (PIV)* and *plastic input displacement (PID)*, respectively.

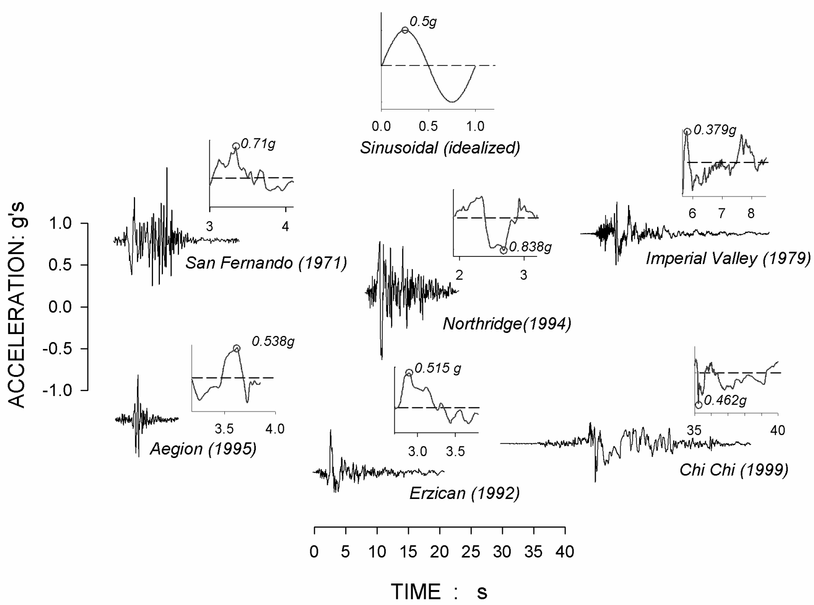

Figure 5. Selected near-field recorded and idealized ground motions containing long-period, high-acceleration pulses.

METHODOLOGY & APPLICATIONS

In applying the above developments, it must be kept in mind that the theory pertains only to yielding response (i.e., where the resistance terms f_y or a_y are constant), thereby identification of the corresponding time intervals is essential. When the excitation contains a large number of high intensity cycles, a numerical approach often provides the only practical means to carry out this task. On the other hand, when only a handful of severe loading cycles exist, the theory can be implemented at a substantially smaller computational effort, possibly by means of hand calculations. This allows valuable insight to be gained on the nature of earthquake demand on yielding structures. An important application, referring to impulsive near-fault earthquake motions, is examined in the ensuing. For simplicity and due to space limitations, the herein reported analyses are limited to rigid-perfectly plastic systems.

With reference to a sliding block on a horizontal frictional plane, six impulsive ground motions affected by forward fault-rupture directivity are employed, as shown in Fig. 5 and Table I. The set encompasses different earthquake motions with peak accelerations (A_g) varying between 0.38 to 1.26g, peak velocities (V_g) ranging from 51 to 263cm/s and peak displacements (D_g) ranging from 9.6 to 430cm. An idealized sinusoidal pulse of full-cycle duration, normalized to 0.5g acceleration, 156cm/s velocity and 78cm displacement (for a total duration of 2s) is also examined. Four yielding acceleration levels (a_y = 0.1, 0.2, 0.3 & 0.4g) are considered, covering a wide range of structural strengths (see also Voyagaki et al 2010).

Table I. Selected near-fault ground motions.

Earthquake	Date	Magnitude M_w	Fault Distance *(km)*	Fault Mechanism[†]	Station	A_g *(g)*	V_g *(cm/s)*	D_g *(cm)*	Bracketed Duration *(s)*
San Fernando, CA, U.S.A.	9/2/1971	6.6	3.0	R	Pacoima Dam	1.23	113	35.4	18.6
Imperial Valley, CA, U.S.A.	15/10/1979	6.5	2.7	S	E05	0.379	90.5	63.1	11.6
Erzican, Turkey	13/3/1992	6.6	2.0	S	ERZ	0.515	84	27.7	13.3
Northridge, CA, U.S.A.	17/1/1994	6.7	6.0	R	Rinaldi	0.838	166	28.2	13.1
Aegion, Greece	15/6/1995	6.3	6.0	N	OTE Building	0.538	51	9.6	5.1
Chi-Chi, Taiwan	20/9/1999	7.6	0.2	O	TCU068	0.462	263	430	24.4

† N: Normal, S: Strike-Slip, R: Reverse, O: Oblique
* HR: Hard Rock, SR: Sedimentary and Conglomerate Rock, SL: Soil and Alluvium

Methodology

Identifying pulse content in an earthquake record is not a trivial task. Alternative proposals have been put forth over the years to determine the initiation and end of these ground excursions by visual and/or computational means (Mavroeidis & Papageorgiou 2003, Bray & Rodriguez-Marek 2004, Baker 2007). Due to a lack of a precise definition for an earthquake pulse and the complexity of the associated time histories, all available methods incorporate some degree of ambiguity. By virtue of the physics of a rigid-perfectly plastic system, a simple unambiguous procedure is employed in this study, as depicted in Fig. 6: *First*, acceleration peaks associated with large velocity content are identified. The initiation of the pulse is set at the time where $\ddot{u}_g=|a_y|$, that coincides with the initiation of yielding and which can be readily established on the acceleration record (point 1, Fig 6a). *Second*, the ordinates and the abscissa of the time history are shifted by a_y and t_y to set the origin of the new axes at the beginning of the pulse (point 1, Fig 6b). *Third*, integration of the modified ground acceleration is carried out considering zero initial conditions, up to the point where plastic input velocity becomes zero. This time instant (point 2, Fig 6b) corresponds to a possible end of yielding and manifests itself in the form of equal areas of opposite signs in the modified record. Peak plastic input velocity and displacement values are traced for the whole time interval. *Fourth*, if the acceleration level in the original record at the zero-velocity time instant is smaller than a_y (not shown in Fig 6), the yielding phase and the associated pulse end, and a new surpass of a_y is sought in the time history. *Fifth*, if the acceleration level in the zero velocity point is larger, in absolute terms, than a_y, the direction of motion of the sliding system reverses and the yielding resistance changes sign. Accordingly, the ordinates of the excitation function are shifted in the opposite direction leading to a jump in plastic input acceleration of $2 \times a_y$ (point 1', Fig 6c). In the proposed procedure, the new phase is treated as an independent pulse, thus integration of the plastic input acceleration is carried out from the new origin of axes considering zero initial conditions until a new zero velocity point is detected (point 4, Fig 6c). *Sixth*, the procedure is repeated until the pulse content of the record is exhausted. *Seventh*, the largest, in absolute terms, maximum ground acceleration and velocity among all individual pulses defines the overall peak values of the plastic input motion. On the other hand, plastic input displacements are cumulative, thereby the overall peak value is obtained by considering the succession of all individual pulse displacements as a single time history. Examples are given below.

The identified pulses can be cast in the form of a single discontinuous excitation function using the ordinates of the first pulse and the abscissa of the original record (Fig 6d). The observed discontinuity between points 2 and 3 is due to the axis shift following the initiation of the second pulse in Fig 6c. Evidently, this is a radically different excitation function as compared to the original time history (Fig 6a), yet it is the one that should be integrated over time for the response of the system. Note that as a consequence of this mathematical operation, the displacement response of the block can be determined as a *linear* process, for the nonlinearity has been embedded into the *PIA* function. More importantly, the latter function may be superior to the original acceleration record in describing the main attributes of seismic demand, for it combines ground acceleration time history with the properties of the yielding system. This sense of linearity however, should be viewed merely as a mathematical vehicle for the response is inherently nonlinear.

It is noted that the procedure for an elastic-perfectly plastic oscillator is analogous to the one described above, with the yielding criterion $|\ddot{u}_g|=a_y$ replaced by the yield condition of the elastic element ($|F(t)| = f_y$) and the equal areas condition in Fig 6 extended to encompass yielding velocity $\dot{u}_y$ (shaded area Fig 3).

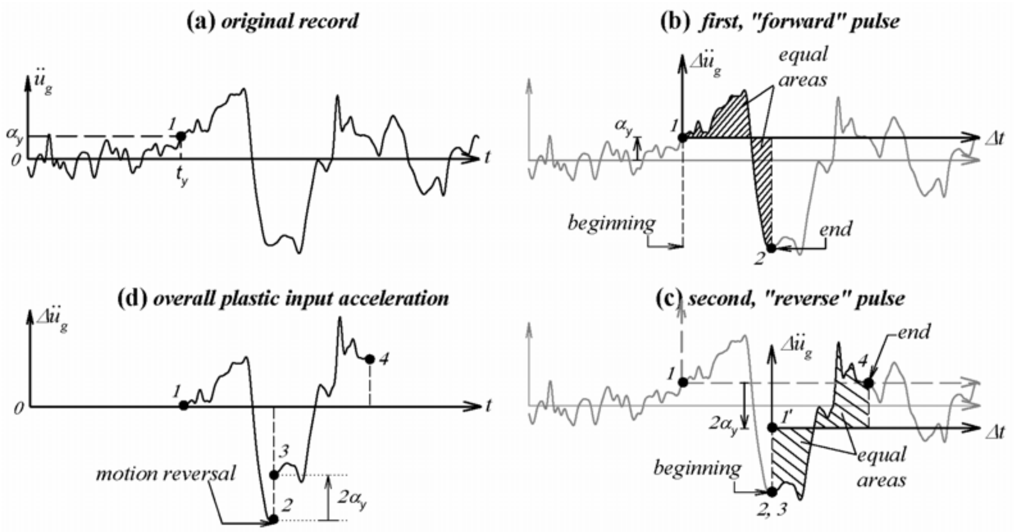

Figure 6. Definition of integration limits and *PIM* according to the proposed approach.

Results

Results for selected ground motions are provided in Figs. 7 to 9, plotted in terms of *PIA* $\Delta\ddot{u}_g(t)$ and its time integrals (i.e., *PIV* and *PID*), for selected values of a_y. Despite significant seismological differences as well as differences in waveforms and intensity among the various motions (Table I), the results for all records exhibit a number of common features: First and foremost, the number of significant pulses varies between 1 and 3, with most motions containing 2 pulses (Table II). Second, the duration of plastic input excitation is limited between about 0.6s (Table II) and 4.2*s* (Fig 7), in sharp contrast with the length of the original records (Table I). Third, all motions containing more than one pulse exhibit characteristic jumps in *PIA* due to alternating signs of yielding resistance between successive pulses (Figs 7, 9). Also, when the conditions of Fig 6c are satisfied, the jumps equal exactly (2 x a_y) as evident in Fig 9. Fourth, peak values of modified ground motion may be significantly lower than in the original ground motion.

Peak values obtained from the above analyses are summarized in Table II, presented by means of the following *peak plastic input motion (PIM)* parameters

$$A_{gp} = \max\left|\Delta\ddot{u}_g\right|,\quad V_{gp} = \max\left|\int \Delta\ddot{u}_g\,dt\right|,\quad D_{gp} = \max\left|\iint \Delta\ddot{u}_g\,dt^2\right| \qquad (24\text{-}26)$$

which are defined over the duration of the pulses in Figs 7 to 9. In the above equations, subscript p stands for "*plastic*".

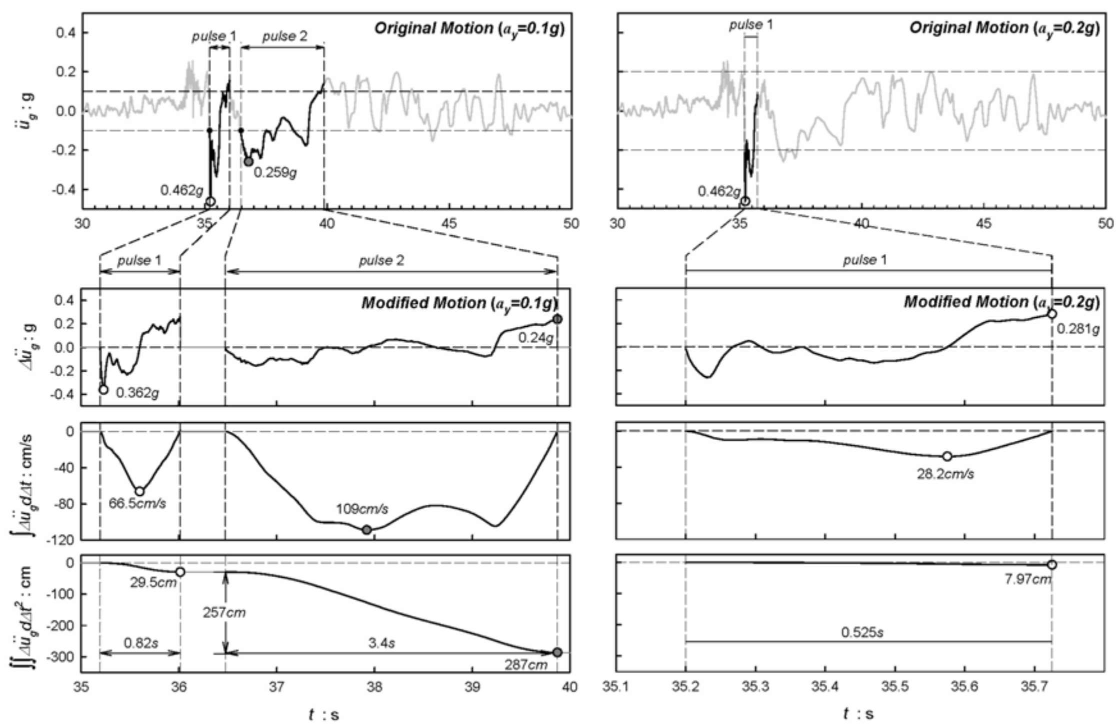

Figure 7. Chi-Chi, Taiwan, 1999, TCU068N record. Plastic input motions for a_y=0.10g & 0.20g.

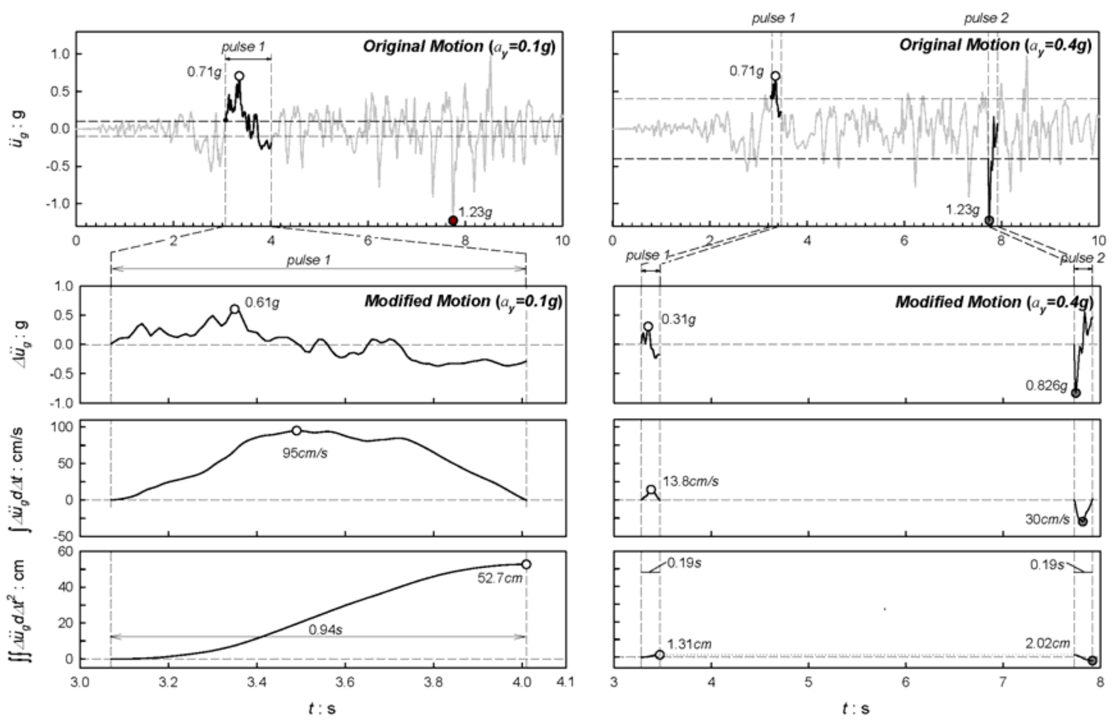

Figure 8. San Fernando, 1971, Pacoima Dam-L record. Plastic input motions for a_y=0.10g & 0.40g.

Evidently, yielding resistance tends to impede *PIM* leading to progressively smaller values of A_{gp}, V_{gp} and D_{gp} with increasing levels of a_y. Interestingly, in a few cases (e.g., Pacoima Dam motion), peak *PIM* are higher than in the original motions. This counterintuitive behavior should be attributed to several factors. For accelerations, this is clearly due to the axes shift, which tends to increase accelerations having the opposite sign of the one originally exceeded at the initiation of the pulse (e.g., Fig 9). On the other hand, for velocities and displacements th,e increase should be sought in differences in initial conditions (e.g., negative initial velocities and displacements in the original ground motion, which do not exist in the modified motions).

Normalized results for different levels of yielding resistance are provided in Fig 10, plotted in terms of ratios A_{gp}/A_g, V_{gp}/V_g and D_{gp}/D_g as functions of normalized strength a_y/A_g. Naturally, for all records these ratios equal 1 for $a_y/A_g = 0$, and 0 for $a_y/A_g = 1$. As mentioned earlier, these ratios generally decrease with increasing levels of a_y/A_g, yet may exhibit values higher than 1 for small values of yielding resistance. The drop in their values reaches dramatic proportions for a_y/A_g exceeding approximately 0.75. Interestingly, the sinusoidal pulse seems to represent quite well the behaviour of the more complex ground motions.

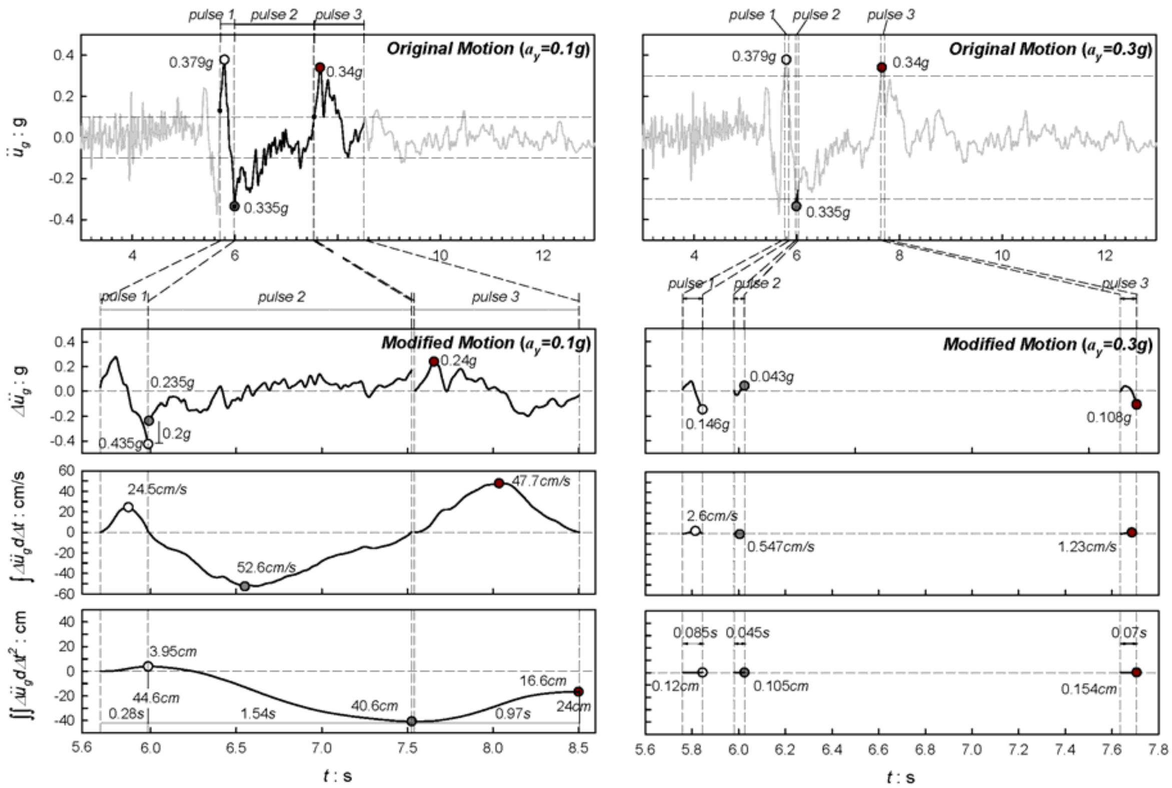

Figure 9. Imperial Valley, 1979, E05-SN record. Plastic input motions for a_y=0.10g & 0.30g.

An interesting set of results is presented in Table II for the case where a_y = 0.1g. Evidently, this is a demanding situation as the yielding resistance is not sufficiently strong to suppress a number of minor pulses present in the accelerograms (see for instance Pacoima record in Fig 8). Two types of analyses are reported here: (A) the simplified analysis presented earlier, based only on the aforementioned major pulses; (B) a rigorous numerical analysis encompassing all the earthquake record, including minor pulses, by means of Eq. (10). The integration limits were specified as depicted in Fig 6, yet the full length of the time history was utilized. With minor exception, the results from the two approaches compare very well, with maximum discrepancies in plastic input velocities and displacements not exceeding 7% and 18%, respectively. In most cases the error is less than 1%. With the exception of Chi-Chi record, the cumulative pulse duration does not exceed 2*s*, a remarkable behavior given the large bracketed duration of the records (Table I). This observation could be potentially useful towards reducing computational effort in dynamic analyses of complex yielding systems.

Table II. Comparison of plastic input peak ground motion parameters considering only major pulses (method A) and by rigorous integration of the whole earthquake record (method B); a_y=0.1*g*.

Ground Motion	(g) (cm/s) (cm)	Method A						Method B	Deviation
		Duration (*s*)	No. of effective pulses	Pulse 1	Pulse 2	Pulse 3	Peak value† (A)	Peak value (B)	(B-A) / B %
Pacoima Dam	A_{ge}	1	1	0.61			0.61	-1.13	46
	V_{ge}			95			95	95.6	0.63
	D_{ge}			52.7			52.7	45	17.1
Imperial Valley	A_{ge}	2.8	3	-0.435	-0.235	0.24	-0.435	-0.435	0
	V_{ge}			24.5	-52.6	47.7	-52.6	-56.7	7.2
	D_{ge}			3.95	-44.6	24	-40.6	-49.3	17.6
Erzican	A_{ge}	0.9	1	0.415			0.415	0.415	0
	V_{ge}			90			90	90	0
	D_{ge}			48			48	48	0
Rinaldi	A_{ge}	1.3	2	-0.867	-0.738		-0.867	-0.867	0
	V_{ge}			127	-102		127	127	0
	D_{ge}			36.1	-34.8		36.1	36.3	0.55
Aegion	A_{ge}	0.6	2	0.56	-0.543		0.56	0.56	0
	V_{ge}			-37.4	36		-37.4	-37.6	0.53
	D_{ge}			-8.5	4.76		-8.5	-8.5	0
Chi-Chi	A_{ge}	4.2	2	-0.362	0.24		-0.362	-0.362	0
	V_{ge}			-66.5	-109		-109	-109	0
	D_{ge}			-29.5	-257		-287	-265	8.3

† Overall peak displacement is defined as the maximum, in absolute terms, considering a succession of all individual pulse displacements as a single time history (Figs 7-9).

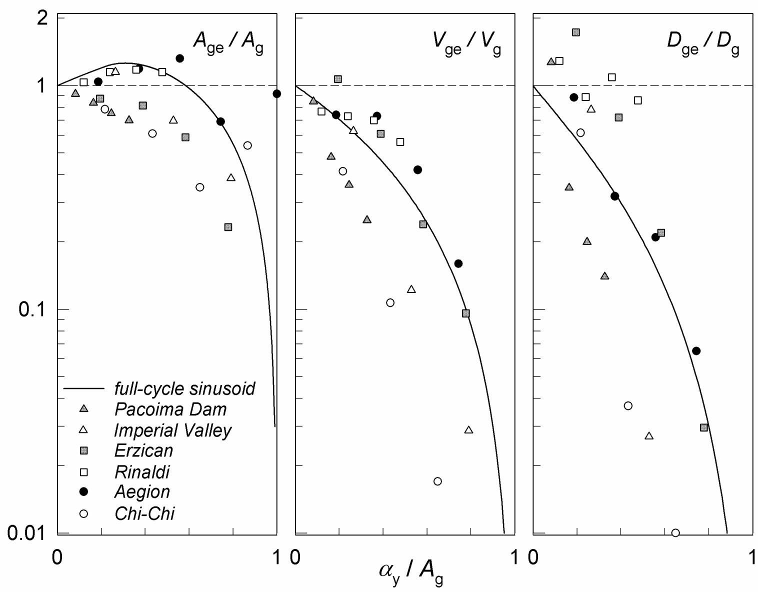

Figure 10. Peak plastic input motion parameters for the waveforms of Fig 5.

CONCLUSIONS

A new set of scaling relations was derived for the response of different classes of yielding systems to dynamic loading. Contrary to classical scaling laws, the derived relations are additive, leading to a shift in the ordinates and the abscissa of the excitation function by an amount equal to the yielding resistance and time of yielding of the system, respectively. By introducing pertinent modified excitation parameters, the response of the system was shown to be obtainable as a linear process. While elements of this approach have long been utilized (notably in sliding block theory), they have not been theoretically investigated and generalized, as done in this work. Peak input motion parameters were determined, encompassing the characteristics of the ground motion and the yielding system. It was shown that these peak ground motions can be substantially (yet not necessarily) smaller than those of the original ground motion. For sliding systems, plastic input acceleration can be interpreted as relative-to-ground acceleration, a parameter that has received less attention as compared to other ground motion parameters in earthquake engineering and seismology. From a practical viewpoint, the derived property can be useful in the case of impulsive excitations, such as near-field earthquake motions affected by forward fault-rupture directivity.

ACKNOWLEDGEMENTS

Financial support to the first Author through *NTUA* Basic Research Program (#65/1720) is acknowledged.

REFERENCES

Baker, J.W. (2007). Quantitative classification of near-fault ground motions using wavelet analysis. Bulletin of the Seismological Society of America. 97 (5): 1486-1501.

Barenblatt, G.I. (1996). Scaling, self–similarity & intermediate asymptotics. Cambridge University Press.

Bracewell, R.N., (1986). The Fourier Transform and Its Applications (second ed.), McGraw-Hill International Editions, New York.

Bray, J.D., Rodriguez-Marek, A. (2004). Characterization of forward-directivity ground motions in the near-fault region. Soil Dynamics & Earthquake Engineering; 24: 815-828.

Chopra, A.K. (2006). Dynamics of Structures. Prentice Hall: Upper Saddle River, NJ

Mavroeidis, G., Papageorgiou, A. (2003). A mathematical representation of near-fault ground motions. Bulletin of the Seismological Society of America; 93 (3): 1099-1131.

Miranda, E., Bertero, V. (1994). Evaluation of strength reduction factors of earthquake – resistant design. Earthquake Spectra; 10 (2): 357-379.

Newmark, N.M., Rosenblueth, E. (1971). Fundamentals of Earthquake Engineering. Prentice Hall: Englewood Cliffs, NJ.

Veletsos, A.S., Newmark, N.M. (1960). "Effect of inelastic behavior on the response of simple system to earthquake motion." Proc. 2nd World Conference on Earthquake Engng, Tokyo, 895-912.

Veletsos, A.S., Ventura, C.E. (1984). Efficient analysis of dynamic response of linear systems, Earthquake Engineering and Structural Dynamics. 12: 521–536.

Voyagaki, E., Mylonakis, G., and Psycharis, I.N. (2010). "A shift approach for the dynamic response of rigid-plastic systems." Earthquake Engineering and Structural Dynamics (accepted for publication).

Voyagaki, E. (2011). Contributions to dynamic analysis of yielding systems to near-fault earthquake motions, forthcoming Ph.D. Thesis, School of Civil Engineering, NTU, Athens